Electronic Supplementary Material (ESI) for RSC Advances.


# A new insight into the transfer and delivery of anti-SARS-CoV-2 drug Carmofur with assistance of graphene oxide quantum dot as a highly efficient nanovector toward COVID-19 by molecular dynamics simulation

Mahnaz Shahabi and Heidar Raissi*

Department of Chemistry, University of Birjand, Birjand, Iran,

*Corresponding author: Email: hraeisi@birjand.ac.ir

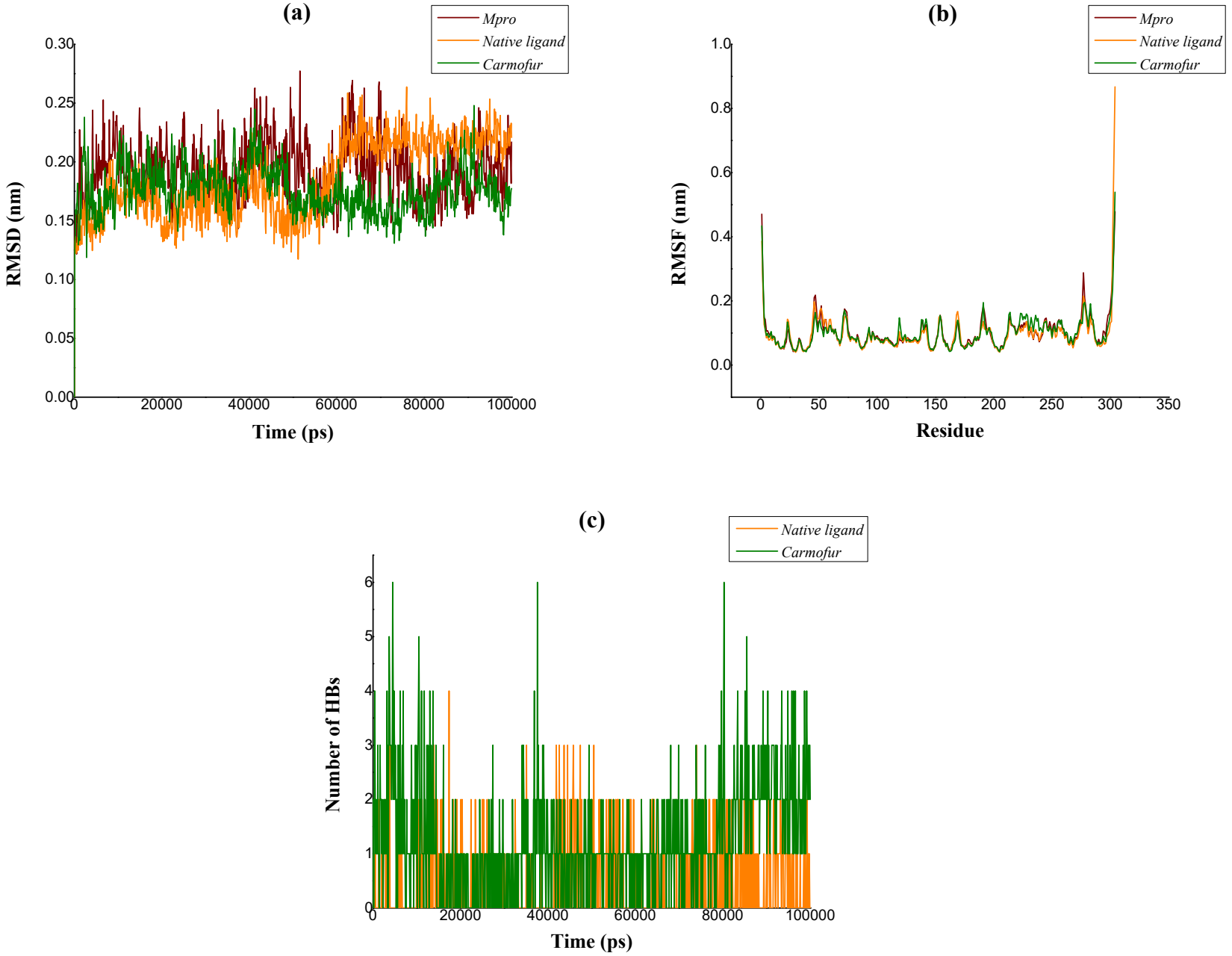
(a)
Mpro
Native ligand
Carmofur
RMSD (nm)
0.00
0.05
0.10
0.15
0.20
0.25
0.30
0
20000
40000
60000
80000
100000
Time (ps)
(b)
Mpro
Native ligand
Carmofur
RMSF (nm)
0.0
0.2
0.4
0.6
0.8
1.0
0
50
100
150
200
250
300
350
Residue
(c)
Native ligand
Carmofur
Number of HBs
0
1
2
3
4
5
6
0
20000
40000
60000
80000
100000
Time (ps)

**Figure S1.** Time evolution of (a) RMSD and (b) RMSF for Cα atoms of main protease with screened compounds and (c) the number of hydrogen bonds between screened compounds and $M_{pro}$ protein.

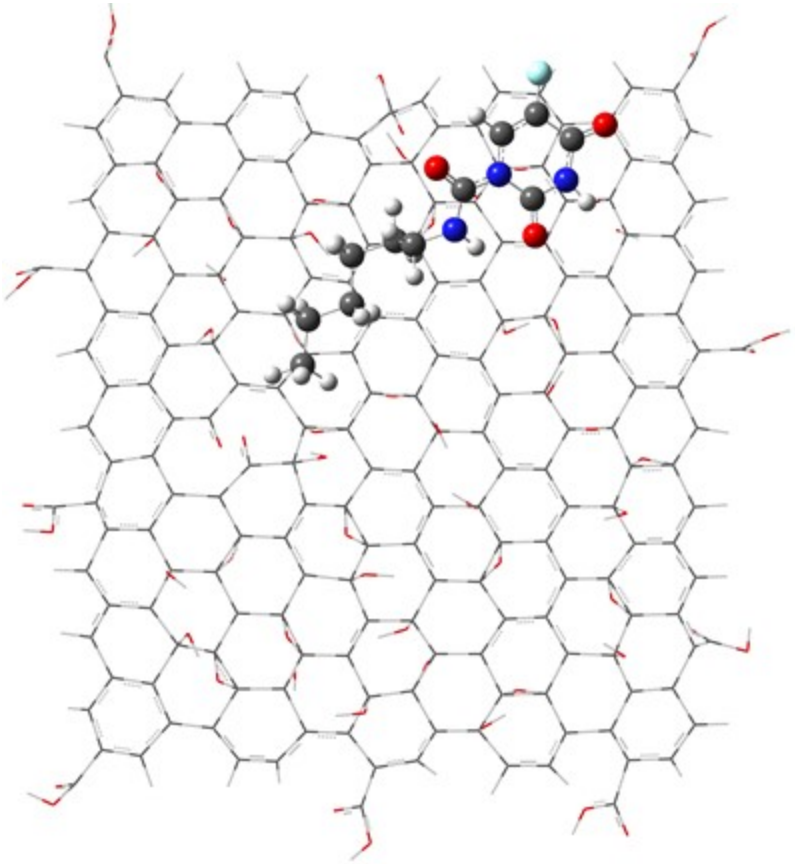

**Figure S2.** Final snapshot of the adsorption of Carmofur on GOQD during 100 ns simulation.

(a)

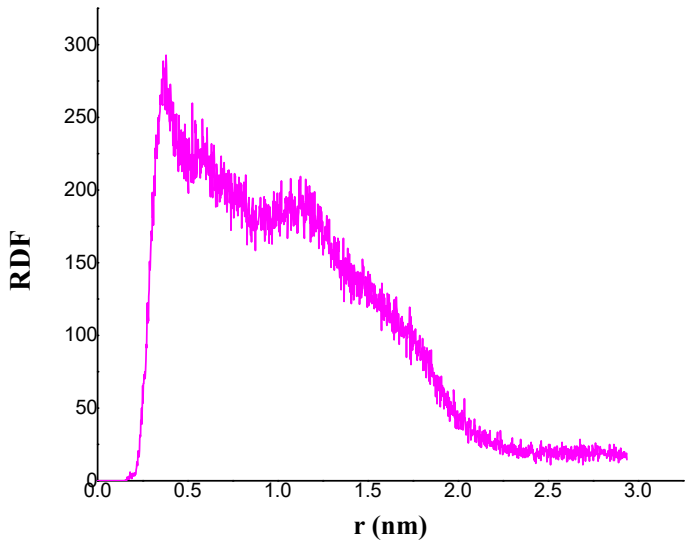
RDF
r (nm)
0
50
100
150
200
250
300
0.0
0.5
1.0
1.5
2.0
2.5
3.0

(b)

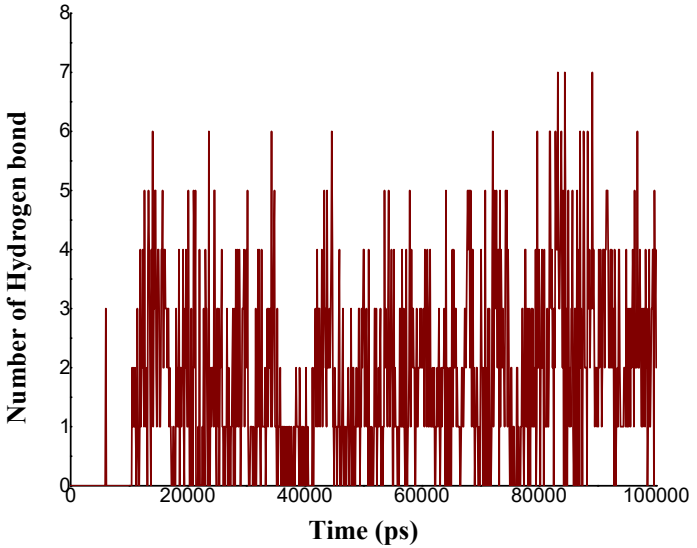
Number of Hydrogen bond
Time (ps)
0
1
2
3
4
5
6
7
8
0
20000
40000
60000
80000
100000

(c)

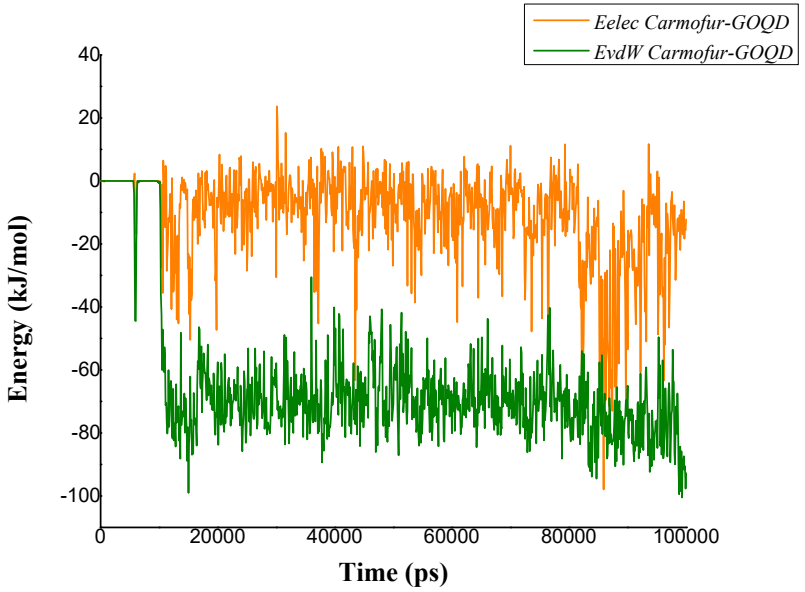
Eelec Carmofur-GOQD
EvdW Carmofur-GOQD
Energy (kJ/mol)
Time (ps)
40
20
0
-20
-40
-60
-80
-100
0
20000
40000
60000
80000
100000

**Figure S3.** (a) Radial distribution functions of Carmofur drug from the surface of the graphene oxide quantum dot, (b) Number of hydrogen bonds and (c) the interaction energy between Carmofur and GOQD.

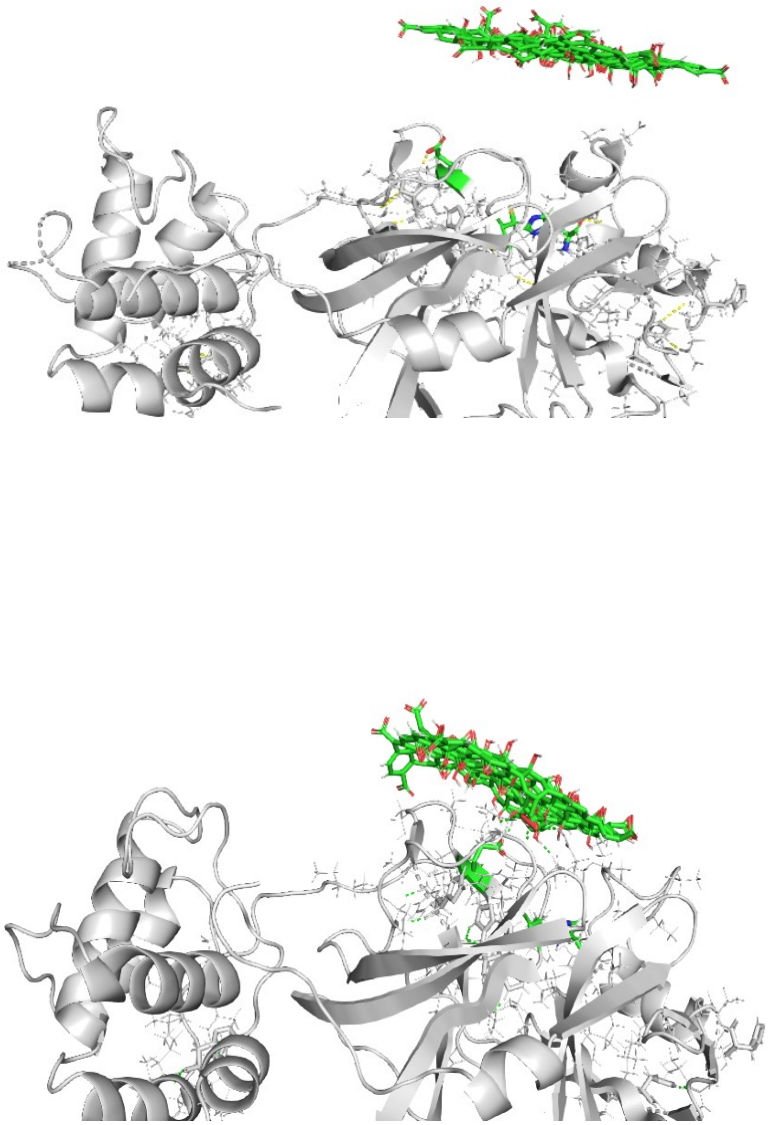

**Figure S4.** Initial (top) and final (bottom) trjectory snapshots for the interaction of GOQD with the binding pocket of Mpro enzyme (Water and ions molecules are not shown for clarity).

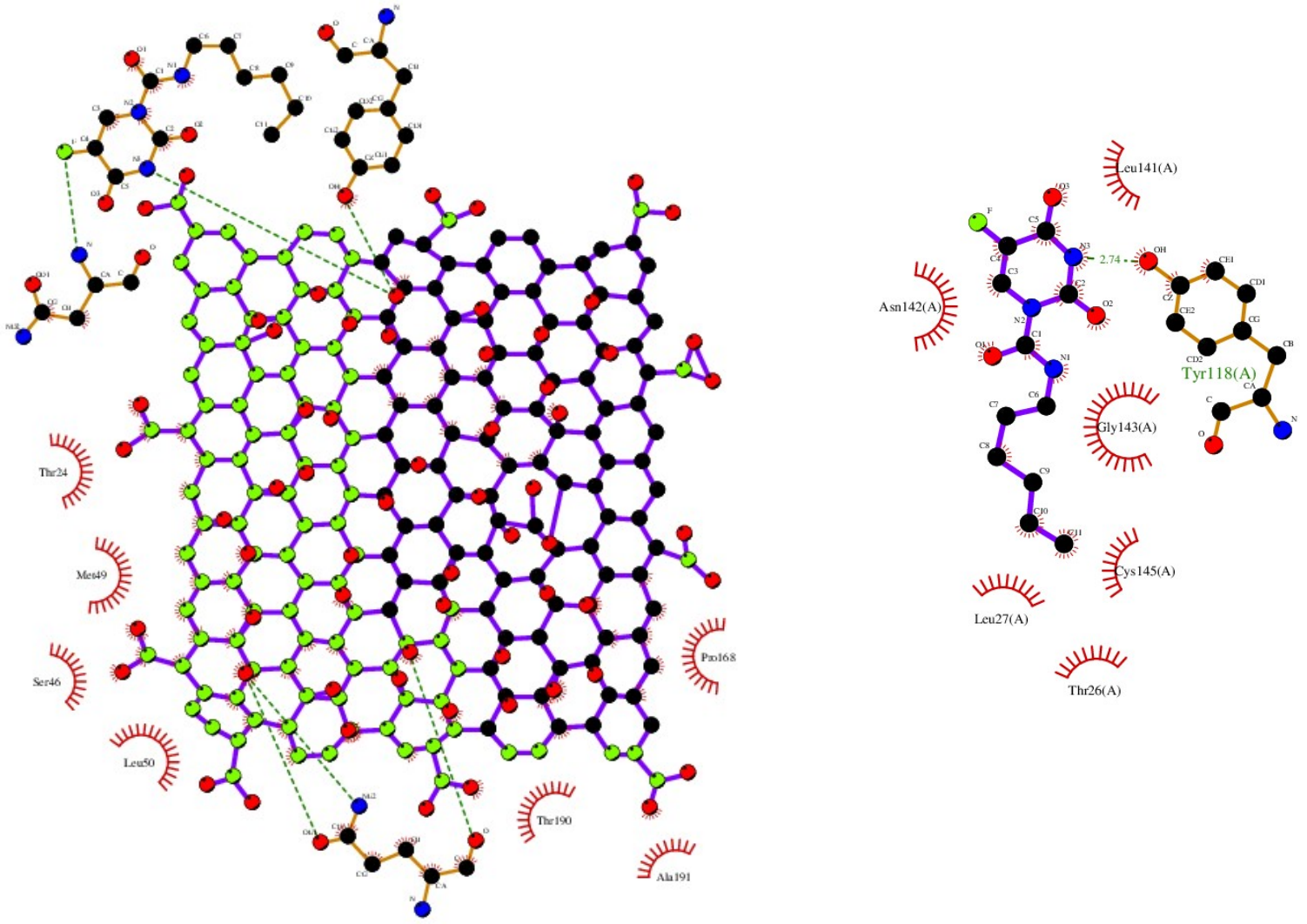


**Figure S5.** 2D interaction of graphene oxide quantum dot (left) and Carmofur (right) with COVID-19 $M_{pro}$ protein during the interaction of complex with the active site of the enzyme.

**Table S1.** Details of the studied systems.

| Description | Composition | Simulation time (ns) | Temperature coupling | Pressure coupling | Simulation cell ($nm^3$) |
|---|---|---|---|---|---|
| $M_{pro}$ enzyme | A box with a $M_{pro}$ protein which in turn is solvated with 29467 water molecules, 89 $Na^+$ and 85 $Cl^-$ ions | 100 | 300K, by Nose–Hoover thermostat | 1 bar, by Parrinello–Rahman barostat | 9.810×9.810×9.810 |
| Carmofur-$M_{pro}$ | A box with a Carmofur-$M_{pro}$ docked model which in turn is solvated with 29444 water molecules, 89 $Na^+$ and 85 $Cl^-$ ions | 100 | 300K, by Nose–Hoover thermostat | 1 bar, by Parrinello–Rahman barostat | 9.810×9.810×9.810 |
| Native ligand- $M_{pro}$ | A box with a native ligand-$M_{pro}$ docked model which in turn is solvated with 29449 water molecules, 89 $Na^+$ and 85 $Cl^-$ ions | 100 | 300 K, by Nose–Hoover thermostat | 1 bar, by Parrinello–Rahman barostat | 9.810×9.810×9.810 |
| Carmofur-GOQD | A box with one Carmofur drug and GOQD which in turn is solvated with 6849 water molecules, 22 $Na^+$ and 20 $Cl^-$ ions | 100 | 310 K, by V-rescale | 1 bar, by Berendsen | 6×6×6 |
| GOQD in complex with $M_{pro}$ | A box with one GOQD and $M_{pro}$ enzyme which in turn is solvated with 29342 water molecules, 91 $Na^+$ and 85 $Cl^-$ ions | 200 | 310 K, by Nose–Hoover thermostat | 1 bar, by Parrinello–Rahman barostat | 9.810×9.810×9.810 |
| Carmofur-GOQD in complex with $M_{pro}$ | A box with one Carmofur drug adsorbed on GOQD and $M_{pro}$ enzyme which in turn is solvated with 29329 water molecules, 91 $Na^+$ and 85 $Cl^-$ ions | 200 | 310 K, by Nose–Hoover thermostat | 1 bar, by Parrinello–Rahman barostat | 9.810×9.810×9.810 |

**Table S2.** The van der Waals ($E_{vdW}$), electrostatic ($E_{elec}$), polar solvation, SASA and binding energy (all in kJ/mol) for the docked compounds into $M_{pro}$ inhibition site during 100 ns simulation.

| | $E_{vdW}$ | $E_{elec}$ | Polar solvation energy | SASA energy | Binding energy |
|---|---|---|---|---|---|
| **Carmofur** | -127.778 ± 0.850 | -29.654 ± 0.518 | 105.862 ± 0.710 | -14.224 ± 0.073 | -65.748 ± 0.756 |
| **Native ligand** | -55.709 ± 0.663 | -8.433 ± 0.622 | 45.843 ± 0.969 | -8.301 ± 0.084 | -26.573 ± 0.480 |